Available online at www.sciencedirect.com
SCIENCE DIRECT®
Journal of Solid State Chemistry 174 (2003) 365–371
JOURNAL OF SOLID STATE CHEMISTRY
http://elsevier.com/locate/jssc

Ion-exchange properties of $P2$-Na_xMnO_2: evidence of the retention of the layer structure based on chemical reactivity data and electrochemical measurements of lithium cells

A. Caballero, L. Hernán, J. Morales,* L. Sánchez, and J. Santos

Departamento de Química Inorgánica e Ingeniería Química, Facultad de Ciencias, Campus de Rabanales, Edificio Marie Curie, Universidad de Córdoba, 14071 Córdoba, Spain

Received 14 November 2002; received in revised form 11 April 2003; accepted 26 April 2003

Abstract

The ion-exchange properties of two $P2$-type layered Na_xMnO_2 bronzes ($x = 0.6$, 0.75) with a differential microstructure were studied in $LiCF_3SO_3$ solutions in acetonitrile under ambient conditions. Na^+ ions are readily exchanged with Li^+, but the reaction causes a significant loss of crystallinity that results in some amorphization. The feasibility of the process increases with increasing structural disorder in the parent compound; conversion, however, is incomplete. The ability of the exchanged material to intercalate water in the air is consistent with the formation of an Li–Mn–O compound that retains the layered framework. Also, the electrochemical data obtained for this material as cathode in lithium cells are consistent with retention of the layer structure and exclude a potential spinel transition due to the ion-exchange reaction. However, the cycling properties of cells made from these layered compounds are quite modest, probably because of the strong structural disorder induced by the lithium reaction.

1. Introduction

$LiMnO_2$ layered oxide has been proposed as a promising candidate cathodic material for secondary lithium cells on the grounds of its high theoretical capacity (285 Ah/kg) and of the fact that Mn is a non-toxic abundant element the compounds of which are more inexpensive than those of Co currently in use [1]. One of the problems hindering its use is the difficulty of preparing them by direct synthesis from lithium and manganese precursors. This has aroused increasing interest in Na–Mn–O phases as Na is larger than Li, which helps stabilize the layered structure. The Li–Mn–O layered phase is thus obtained via a topotactic exchange reaction with Li^+ that essentially maintains the original layered lattice.

Na_xMnO_2 layered bronzes exhibit three types of structure, namely: $P3$, $O3$ and $P2$ (where P and O denote trigonal prismatic and octahedral geometry, respectively, and the figure following them the number of MnO_2 sheets forming the unit cell) [2]. The earliest phase synthesized on purpose with a view to its subsequent ion exchange was α-$NaMnO_2$, which possesses an $O3$ structure. Following ion exchange, an $LiMnO_2$ phase that retained the $O3$ structure was obtained [3,4]. The most serious problem of this layered phase arises from its structural instability during the electrochemical insertion and extraction of lithium. By cycling over the 3–4 V range, the material is converted into a spinel structure [5] and cell performance is degraded as a result. Paulsen et al. [6] noted that the $P2$ phase is a unique phase the structure of which is not related with the spinel. Two different phases related with the $P2$ model have been reported for Na_xMnO_2 bronzes, [7] namely: (a) an oxygen-rich phase labelled α-$Na_{0.7}MnO_{2+y}$ ($0.05 \leqslant y \leqslant 0.25$), indexed in the hexagonal system and stable at low temperatures; and (b) a β-$Na_{0.7}MnO_{2+y}$ phase ($y \leqslant 0.05$) indexed in the orthorhombic system, possessing a lower oxygen content and obtained at high temperatures. Recently, Paulsen and Dahn [8] revisited these systems, and starting from Na_2CO_3 and MnO_2 (electrolytic manganese dioxide) and heating at 1000°C, they obtained a phase named HT-$P2$-$N_{2/3}MnO_2$ indexed in a monoclinic cell. Below 600°C, they obtained a poorly crystalline compound

*Corresponding author. Fax: +34-957-218621.
E-mail address: iq1mopaj@uco.es (J. Morales).

0022-4596/03/$ - see front matter © 2003 Elsevier Inc. All rights reserved.
doi:10.1016/S0022-4596(03)00247-0

named LT-$Na_{2/3}MnO_2$ the XRD pattern for which that was indexed in the hexagonal system, even though some typical reflections were absent. Both phases undergo ion exchange with lithium ions under mild conditions; the reaction shifts the oxygen stacking layers and yields *O*2-$Li_{2/3}MnO_2$ phases that retain the layer network. The main difference is the stronger tendency of the low-temperature phase to yielding a pure Li_xMnO_2 compound.

The ion-exchange results obtained by Jeong and Manthiram [9] for a hexagonal undistorted *P*2 phase of $Na_{0.7}MnO_{2+y}$ ($y \approx 0.3$) composition contradict the previous description. According to these authors, the ion-exchange reaction of the hexagonal form yield the spinel $LiMn_2O_4$ or a lithiated spinel ($Li_2Mn_2O_4$).

Recently, we developed a synthetic method for preparing hexagonal highly crystalline *P*2-$Na_{0.6}MnO_2$ stable at high temperatures [10]. In order to shed some to light over this controversy, in this work we explored its ion-exchange properties. The comparative study of the electrochemical properties of the parent and exchanged phases as cathodes in lithium cells is highly illustrative as a tool for settling this controversy.

2. Experimental

Na_xMnO_{2+y} bronzes were obtained by a sol–gel method using propionic acid as the resin framework [11]. The experimental conditions, used and the chemical and structural characterization methods employed are described in detail elsewhere [10]. The most salient feature of these bronzes is their ability to retain the hexagonal network at temperatures as high as 800°C.

The ion-exchange reactions were carried out at ambient temperature by stirring with a fourfold excess of a $LiCF_3SO_3$ solution in acetonitrile for 24 or 48 h. The chemical was supplied by Strem Chem. The products formed in the ion-exchange reactions were filtered, washed with acetonitrile, dried in vacuo and stored in an M-Braun glove box. The average oxidation state of Mn (AOS) was measured by dissolving the sample in dilute sulfuric acid containing a known excess of Fe^{2+} under a continuous flow of argon. Unreacted Fe^{2+} was titrated with a 0.01 M $KMnO_4$ solution previously standardized with $Na_2C_2O_4$. The total Mn, Na and Li contents were determined by atomic absorption spectroscopy (AAS).

X-ray powder diffraction (XRD) patterns were recorded on a Siemens D-5000 diffractometer using monochromatic Cu*K*α radiation. Because the samples reacted with moisture, a piece of Mylar plastic was used to isolate the powders.

Electrochemical measurements were carried out in two-electrode cells, using Li (supplied by Strem) as anode. Powdered pellets 7 mm in diameter were prepared by pressing, in a stainless-steel grid, ca. 10 mg of active material with graphite (7.5 wt%), acetylene black (7.5 wt%) and PTFE (5 wt%). The electrolyte, supplied by Merck, was 1 M anhydrous $LiPF_6$ in a 1:2 mixture of ethylene carbonate and diethyl carbonate. Cells were assembled in an M-Braun glovebox. Cyclic voltammetry was performed with a Solartron 1286 Electrochemical Interface controlled via the CorrWare and CorrView software packages, run on a PC 486 computer. Curves were recorded at a scan rate of 50 μV/s. Cycling tests were performed in the galvanostatic mode and controlled via a multichannel MacPile potentiostat–galvanostat.

3. Results and discussion

Two samples were prepared from the gels fired at 800°C, starting from a different Na/Mn ratio. By combining the AOS and the amount of Na and Mn obtained by AAS the following nominal compositions were calculated: $Na_{0.6}Mn_{1.07}O_{2.05}$ (AOS 3.3) (henceforward sample A) and $Na_{0.75}Mn_{1.05}O_{2.02}$ (AOS 3.1) (sample B). The XRD patterns for the two samples are shown in Figs. 1a and b. All reflections for sample A were indexed in the hexagonal system (*P*2 structural model); on the other hand, the pattern for sample B included several weak peaks that could not be indexed in this system. Moreover, the latter sample exhibited broader peaks [particularly those with (0*kl*) indexes], which suggests higher structural disorder. These results

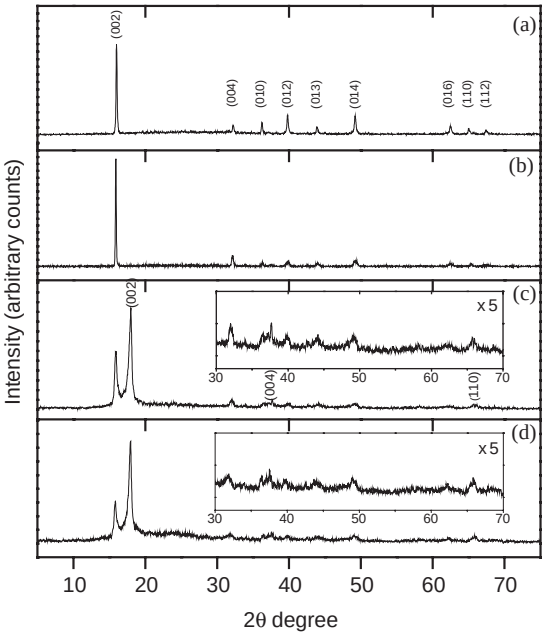

Fig. 1. XRD patterns for as-prepared samples [(a) sample A, (b) sample B], following ion-exchange with $LiCF_3SO_3$ in acetonitrile for 24 h [(c) sample A, (d) sample B].

simply reflect one peculiarity of the Na_xMnO_2 layer bronze, namely: that subtle changes in the experimental conditions considerably affect the final microstructure. The more crystalline compound (sample A), was refined by the Rietveld method in the space group $P6_3/mmc$, [10] with unit-cell dimensions $a = 2.8603(4)$ Å, $c = 11.153(2)$ Å. The structural model is consistent with the *P*2-type structure with an ABBA staking sequence for oxygen layers; the octahedral and trigonal prismatic sites formed being occupied by Mn and Na ions, respectively.

The two compounds were subjected to ion-exchange reactions under mild conditions aimed at preparing Li–Mn–O layered phases in order to avoid the transformation into a spinel framework. According to Paulsen et al. [6], such a transformation involves a rearrangement of the oxygen lattice with cleavage of all Mn−O bonds. This seems to be highly unlikely at room temperature. In fact, the ion exchange of this phase in LiBr at 180°C clearly led to the formation of $LiMn_2O_4$ [9]. The XRD patterns for the exchanged samples are shown in Figs. 1c and d. All share several features. One is the presence of a new, strong peak at ca. 18° (2θ) the spacing of which (4.84 Å) is somewhat smaller than the repeat distance (5.62 Å) of the Na-containing precursor and associated to the (002) reflection. The intensity of this latter reflection decreases with increasing reaction time, the ion exchange being faster at the beginning of the process. However, the peak does not completely disappear and conversion is incomplete. In fact, increasing the Li/Na atom ratio or the reaction time by a factor up to 8 only resulted in stronger amorphization. The ion exchange also causes an appreciable loss of crystallinity, even after short times (24 h) (Fig. 1c); this adds some difficulty to the identification of the new phase formed. Nevertheless, in addition to weak and broad peaks coinciding with those for the parent compound, the ion-exchanged products exhibit at least three distinct reflections at 4.841, 2.395 and 1.417 Å. This allowed the XRD pattern for the new phase formed to be indexed in the hexagonal system rather than the cubic system, with the following unit-cell dimensions: $a = 2.835(2)$ Å and $c = 9.63(1)$ Å. These data are better explained by assuming the formation of a Li_z MnO_2 layered phase—a *P*2 to *O*2 transformation, as suggested by Paulsen et al. [6]—rather than a $Li_2Mn_2O_4$ lithiated spinel as claimed by Jeong and Manthiram [9] based on measurements similar to those carried out in this work. As shown below, this assumption is also supported by electrochemical results. In addition, the ion exchange is more favorable in the sample B, which also exhibits higher disorder (Fig. 1d). In this case, the $I_{Na(002)}/I_{Li(002)}$ ratio was 0.40 rather than 0.58 as calculated for the sample with a lower sodium content (Fig. 1c). This is consistent with the results of Paulsen et al. [6]; however, we failed to obtain an Li_xMnO_2 single phase ($x = 0.6$; 0.75). Nor was a $Li_yNa_{x-y}MnO_2$ intermediate phase with a layer spacing in between those of *P*2-Na_xMnO_2 and Li_xMnO_2 obtained under the experimental conditions used. This result is consistent with the differences in size and coordination between lithium and sodium ions. In fact, the interlayer spacing of the Li-based compound is smaller than that of the Na compound. The chemical analysis of the sample exhibiting the higher conversion yielded an overall composition $Na_{0.23}Li_{0.62}Mn_{1.08}O_2$ (AOS 3.0). The presence of Na is consistent with the partial conversion observed by XRD. On the other hand, the topotactic character of the ion-exchange reaction reflects in the shape and morphology retention of the particles after the reaction. Thus, the particles of the parent compound, sample B, exhibit a lamellar morphology with a highly uniform size of 3–5 μm (Fig. 2a). Particle shape is more uneven than in sample A, which is consistent with its higher crystallinity [10]. After the exchange reaction, the morphology is retained and the particles differ little from those of the parent compound (Fig. 2b).

Indirect evidence of the formation of a layered lithiated phase was obtained from the reaction undergone in contact with air for 3 weeks (see Fig. 3a). The

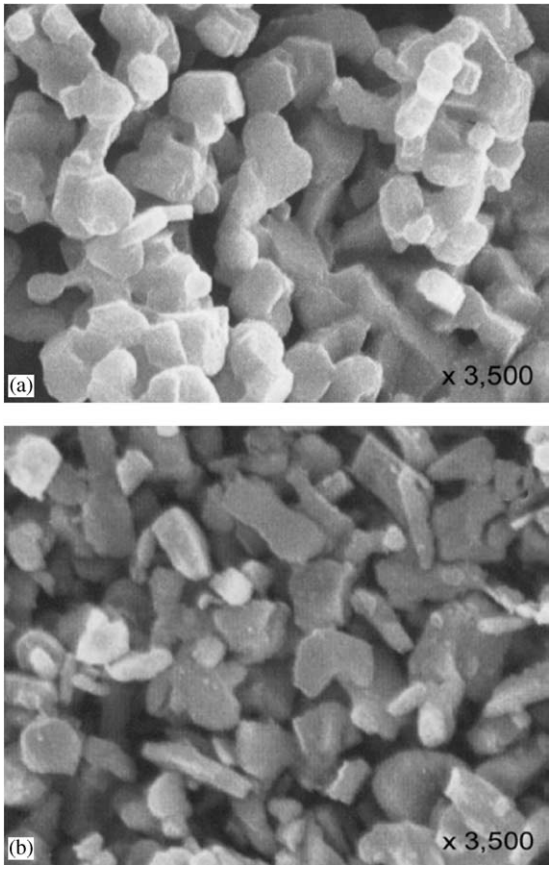

Fig. 2. Scanning electron micrographs of sample B before (a) and after the ion-exchange reaction (b).

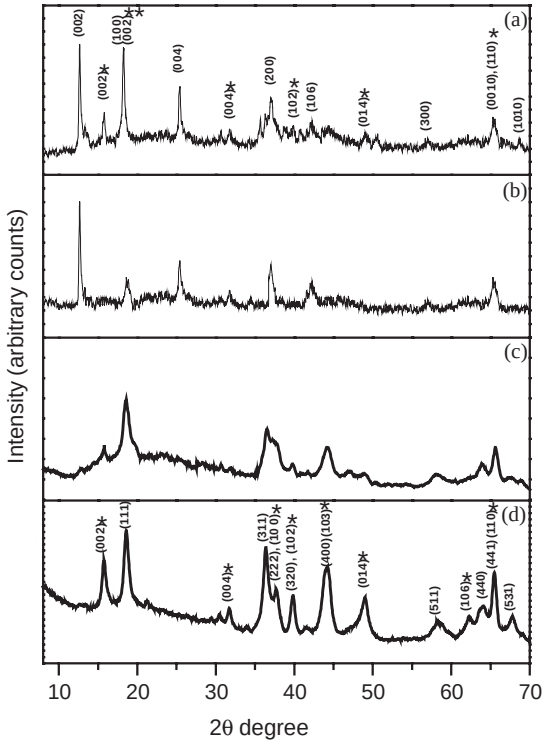

Fig. 3. XRD patterns for the ion-exchanged sample A (a) exposed to air for 3 days; (b) after heating at 60°C at 98% relative humidity for 6 days; (c) and (d) after recording the thermogram up to 180°C and 400°C, respectively [(*), (**) reflections belonging to Na and Li phases, respectively].

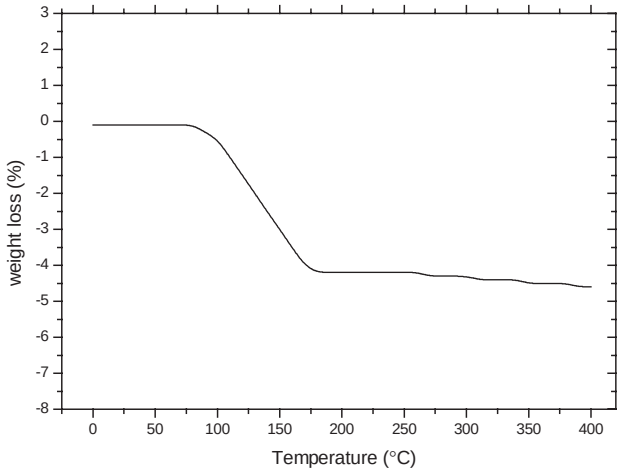

Fig. 4. Thermogravimetric curve for the ion-exchanged sample B exposed to the air for 3 days.

compound thus obtained exhibits a strong peak around 7.0 Å, typical of the interlayer spacing of the birnessite group in lamellar MnO_2 [12]. This peak, together with those at 3.50, 2.42 and 2.12 Å, can be indexed in a hexagonal unit system, with cell dimensions $a = 5.59$ Å and $c = 7.06$ Å, which are quite consistent with a birnessite-type structure [13]. In addition to these new peaks, the most salient signals at 5.61 and 4.84 Å, which belong to the layered phase of Na and Li, respectively, are still present and in a similar intensity ratio. However, there is still the additional difficulty of interpreting the pattern as a result of the birnessite structure having a plane of low intensity assigned to (100) at 4.84 Å, which is nearly identical with the basal spacing of the Li phase. Treating this sample at 60°C at a constant relative humidity of 98% for 6 days, shed some light on the origin of this peak. Thus, the intensity of the peak at 4.84 Å was significantly decreased and the peak associated to the Na phase disappeared (see Fig. 3b). On the other hand, the peaks belonging to a hydrated system hardly changed. These results can be more accurately interpreted by assigning the peak at 4.84 Å to the Li phase. Moreover, the compound is highly resistant to hydration, taking into account the drastic conditions used to promote the reaction. One open question is the difficulty in discriminating the Li- and Na-containing hydrated phases as the peak at 7.01 Å does not split into two with different interplanar distances. It seems plausible that a differential water content in the interlayer may offset the difference in size between Li and Na ions. In fact, the difference in interlayer spacing between Na- and Li-birnessite is only 0.1 Å. The thermogravimetric analysis of the sample with the highest conversion, Fig. 4, revealed a weight loss of 4.2% over the temperature range 100–180°C and was ascribed to the release of interlayer water, consistent with the XRD pattern (see Fig. 3c). The peaks belonging to the hydrated system are lost, but the pattern cannot be indexed in a mixture of Na and Li phases. Although the main peaks for the Na phase are still present, the remaining reflections are better indexed in a cubic symmetry (a spinel-type structure). Further heating hardly affects the sample weight, but crystallinity is clearly improved, as reflected in the better defined reflection lines (Fig. 3d). Thus, the water loss induces a structural transformation, viz. the conversion of the layered lithiated phase into the spinel-type structure, which is the more stable structure for the Li–Mn oxides [14]. All these results reveal that *P*2-Na_xMnO_2 treated in $LiCF_3SO_3$ undergoes an exchange reaction but retains the oxygen layer network. These phases have the ability to slowly react with water and retain the layer structure with the alkali ions and water sharing the interlayer spacing [13].

Two samples were selected with a view to examining the electrochemical behavior in lithium cells, namely: (a) the untreated sample A with a *P*2 structure and (b) that exchanged with lithium at maximum conversion, of nominal composition $Na_{0.23}Li_{0.62}Mn_{1.08}O_2$, the main component of which was an Li–Mn layered bronze (Fig. 1d). The cyclic voltammograms for lithium intercalation into the two samples exhibited a significantly different behavior (Figs. 5a and b). Thus, the cathodic curve for

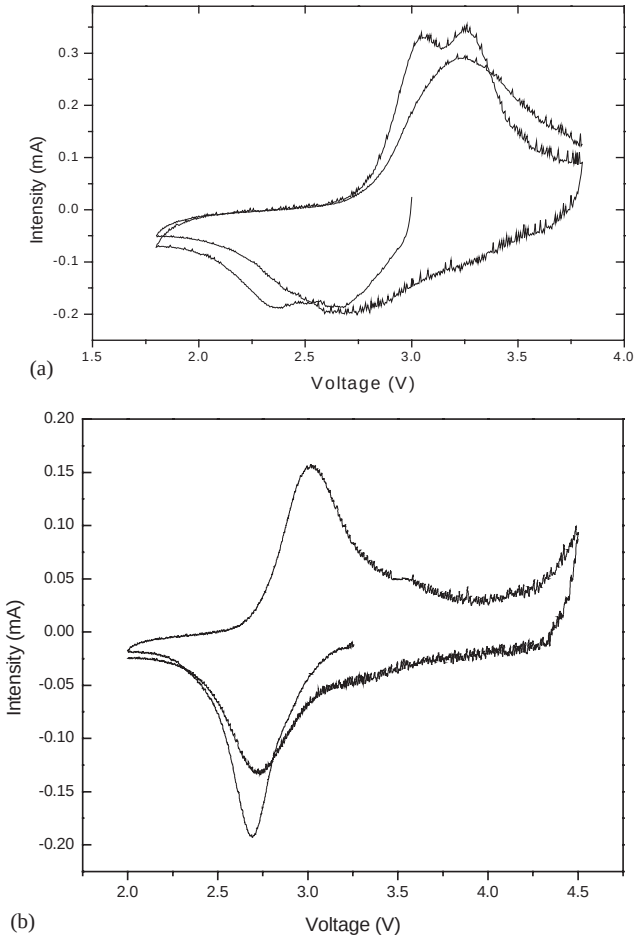

Fig. 5. Cyclic voltammograms for sample A before (a) and after the ion-exchange reaction (b).

$Na_{0.6}MnO_2$ exhibited a broad signal with two components centered at 2.67 and 2.37 V, respectively. The anodic wave had a similar shape; it consisted of: two well-defined peaks at 3.05 and 3.25 V. These results differ from those reported by Kim et al. [15] for $K_{0.3}MnO_2 \cdot 0.1H_2O$, a compound with a *P*2-type structure. In this system, both the discharge and the charge curves are consistent with a single-step reaction. However, the same research group [16] obtained a charge curve resolved into two peaks for $Li_{0.12}K_{0.35}MnO_{2.14} \cdot H_2O$ with a *P*2-type layered structure at 3.18 and 3.79 V, the latter of which was ascribed to the oxidation of interlayer water molecules. We can think of no plausible explanation for the two steps observed in lithium insertion and extraction. A model based on the two available prismatic sites being partially occupied by Na^+ ions would be inconsistent both with lithium coordination and with energy considerations. Moreover, although the reduction–oxidation process seems to be reversible judging from the likeness of the cathodic and anodic waves, hysteresis in the peaks is quite significant (0.68 and 0.58 V for the low- and high-voltage peak, respectively). This suggests that the host undergoes substantial structural changes. In fact, the *P*2-based structure was heavily distorted upon lithium insertion (Fig. 6a) and tended to collapse after the reduction–oxidation process (Fig. 6b). However, a weak, ill-defined peak at ca. 4.83 Å was detected throughout the basal spacing of which was similar to that observed in the chemical ion-exchange reaction. This means that the electrochemical insertion of lithium also tends to promote a structural rearrangement to yield a Li layer phase, albeit with a high disorder. This sample is highly reactive and readily uptakes water, even on standing covered with the Mylar film (Fig. 6c). The cyclic voltammogram for the second discharge reflects this loss of the *P*2 structure and exhibits only a broad peak centered at 2.6 V. This single peak is the main feature of the second charge curve and is retained on further cycling. The *quasi*-amorphous state of the active material could be used to explain the differential shape of the curves compared with those for the first cycle.

In contrast with the electrochemical behavior exhibited by the untreated sample, the curve for the

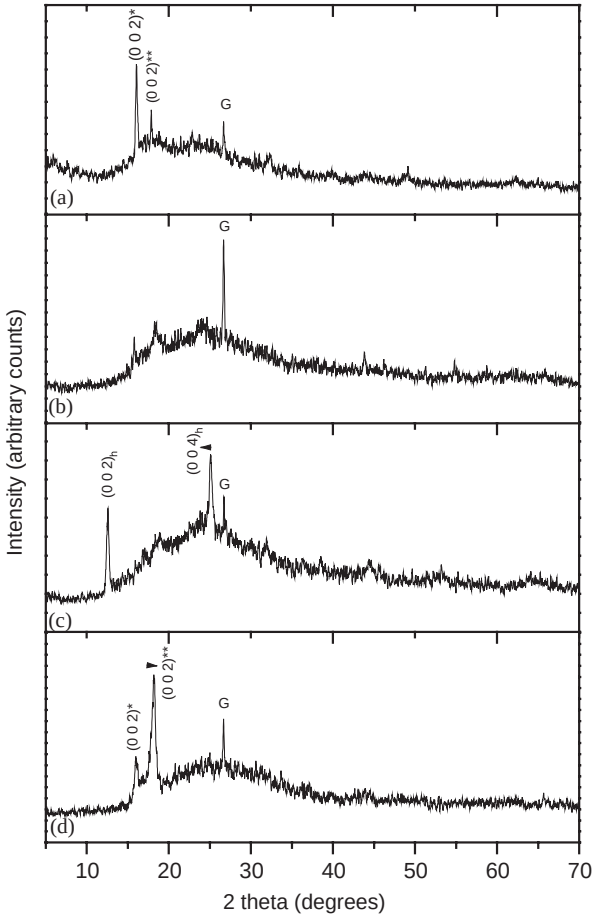

Fig. 6. XRD patterns for sample A obtained at different stages during the lithium insertion process, discharged at 1.8 V (a) then charged to 3.8 V (b), and after exposure to air (c). (d) Ion-exchanged sample discharged at 1.8 V [reflections marked with (G), (*), (**) and (h) belong to graphite, Na, Li and hydrated phases, respectively].

exchanged sample (Fig. 5b) exhibits a broad, symmetric cathodic peak centered at 2.67 V, and the anodic wave a somewhat more asymmetric peak at 3.1 V. On further discharge, the cathodic peak becomes weaker, broader and more asymmetric, and shifts to 2.82 V, whereas the voltage of the anodic peak hardly changes. Upon cell cycling, the single redox pair is maintained, so it does not split into two peaks as in $Li_xMn_2O_4$ spinel electrodes [17]. Two findings are thus worth noting. First, the cyclic voltammograms for the exchanged sample are better interpreted in terms of a layered Li–Mn–O system rather than a spinel-type structure. Second, the material does not become a spinel phase on cell cycling. In fact, the structure of the discharged sample up to 1.8 V hardly changes with respect to the original sample (Fig. 6d).

The voltage profiles for the first few discharges and charges, recorded by using a current density of $0.25\,mA/cm^2$ in the galvanostatic mode, are shown in Figs. 7a, and b. The initial open-circuit potential for sample A was around 3.2 V; about 0.43 mol of lithium per formula unit can be incorporated into the structure at the first discharge at a cut-off voltage of 2.2 V. This value is consistent with structural and composition criteria as the maximum Li uptake should be around 0.4 mol per formula unit, thus filling all the empty trigonal prismatic sites available if the hypothetical, but unlikely, model of structure retention is assumed. In any case, the amount of lithium extracted by charging up to 3.8 V coincides with that electrochemically inserted. The

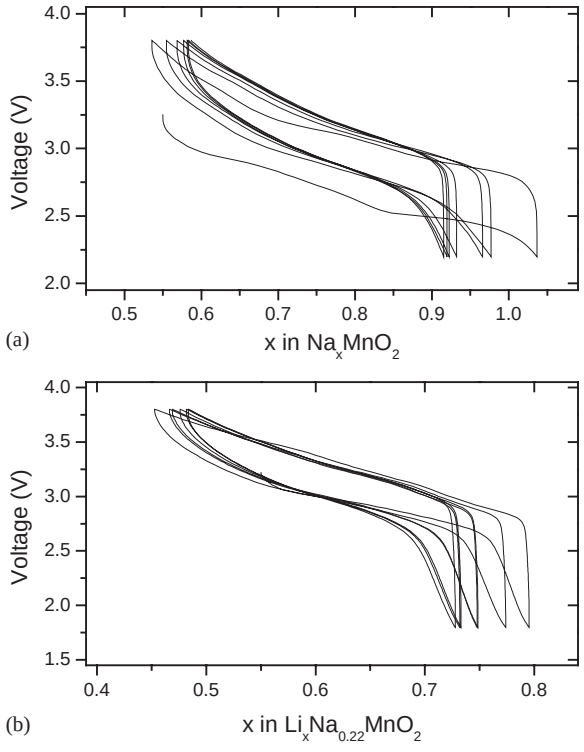

Fig. 7. Charge–discharge curves for sample A (a) and the ion-exchanged sample (b) in lithium cells.

first discharge and charge curves are consistent with the cyclic voltammogram profile: the two *pseudo*-plateaux observed suggest that the lithium reaction takes place in at least two steps. Both the discharge and the charge profiles obtained on further cycling are consistent with a single-step reaction and hence with the single peak observed in the voltammogram.

The galvanostatic discharge/charge profile for the exchanged sample differs from those observed for sample A and the spinel-related phases. First, the initial discharge capacity is very short (only 0.25 mol of lithium is incorporated into the structure at a cut-off voltage of 1.8 V). The origin of this reduced capacity is difficult to trace owing to the uncertainty in the sample composition. Second, the discharge and charge curves are smooth and exhibit no plateau. This is consistent with the cyclic voltammogram containing a single peak and rules out a spinel transformation. On charging the cell up to 3.8 V, one can extract ca. 0.5 mol of lithium (including that electrochemically inserted). However, the curve profile does not allow one to distinguish between chemically and electrochemically inserted lithium, which suggests that both types of lithium occupy energetically equivalent positions in the layer framework. In fact, as shown by the XRD pattern (Fig. 6d) electrochemically inserted lithium introduces minimal changes in the structure: a peak shift from 4.84 to 4.80 Å. This lattice contraction is consistent with the layered structure because an increased lithium content should strengthen the binding between the pillaring cations and the negatively charged oxide layer.

With regard to the cycling properties of these electrodes, Figs. 8a and b show the specific capacity of the cells as a function of the number of cycles. The initial capacity delivered by the cell formed with $Na_{0.6}MnO_2$ was 150 mAh/g, but decayed slowly on further cycling. After the tenth cycle, the capacity was still maintained but had dropped to nearly 50% of the initial value and the cell could only deliver about 80 mAh/g. This value is lower than that obtained for $K_{0.30}MnO_{2.11}\cdot 0.6H_2O$ [15], which delivered an initial capacity of 175 mAh/g and retained more than 75% of it after 50 cycles. The promising electrochemical behavior of this material is rather surprising as it contains water molecules that ought to have an adverse effect on the cell (simply via hydrolysis reactions). If the cell made from the exchanged sample was initially discharged to 1.8 V and then charged to 3.8 V, approximately 140 mAh/g could be removed. About 120 mAh/g was inserted into the cathode in the following discharge. Unfortunately, the cell capacity continuously faded with cycling (Fig. 8b); after 20 cycles the cell had lost over 50% of its initial capacity. This cell performed somewhat worse than that of the cell based on the unexchanged sample, notwithstanding the apparent greater simplicity of the lithium reaction and the lesser structural changes required to

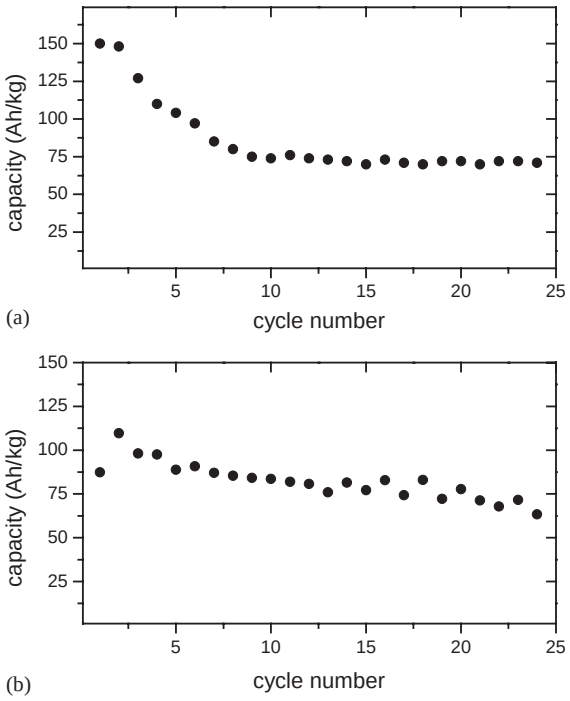

Fig. 8. Variation of the specific capacity with the number of cycles. (a) Sample A (voltage window 3.8–2.8 V). (b) Ion-exchanged sample (voltage window 3.8–1.8 V).

accommodate the lithium. Subtle changes in some parameters are not always easy to control; thus, the degree of purity and composition uniformity, those of crystallinity and structural disorder, particle morphology and size distribution, can affect the cycling properties of the cell.

4. Conclusions

Of the three mechanisms proposed to account for the ion-exchange properties of *P*2-type layered Na_xMnO_2 in contact with lithium salts under mild conditions [viz. (a) a simple ion exchange that preserves the oxygen stacking sequence and where Li^+ and Na^+ coexist; (b) a change in oxygen stacking that preserves the layer structure, with Li^+ ions occupying octahedral positions, and a *P*2 to *O*2 transformation; and (c) a rearrangement of the oxygen lattice to a spinel-like phase], the second is the most consistent with the results obtained in this work. As regards the first mechanism, no $Li_yNa_{x-y}MnO_2$ phase with a basal spacing in between those of Na (5.62 Å) and Li (4.93 Å) phases, was detected, whatever the degree of conversion. This is consistent with the differential preferred coordination of Li^+ (octahedral) and Na^+ (trigonal prismatic) ions. Discriminating the other two models is troublesome because the strongest peaks in the XRD patterns for the Li phase (*O*2-type structure) and $LiMn_2O_4$ or $Li_2Mn_2O_4$ (spinel structure) are nearly identical; also, the phases obtained are poorly crystalline. However, the difference in structure type results in a distinct reactivity. Thus, the exchanged phase reacts readily with water and yields a Li birnessite-type structure. This process can be easily interpreted as the intercalation of water in the interlayer spacing of a layered phase such as Li_zMnO_2. Also, the reactivity toward lithium as examined in lithium cells is highly illustrative of the adoption of a layered structure. Thus, the cyclic voltammogram exhibits a single peak rather than the two well-known peaks for spinel-related phases. However, the reaction of Na_xMnO_2 *P*2-type bronzes with lithium, either in solution or electrochemical, induces significant structural disorder and tends to yield amorphous particles. This may be the reason for the their limited ability as cathodes in Li secondary batteries.

Acknowledgments

Financial support from Junta de Andalucía (Group FQM 175) and Spain's Ministry of Science and Technology (Project MAT2002-04477-C02-02) is gratefully acknowledged.

References

[1] T. Nagaura, K. Tozawa, Prog. Batt. Solar Cells 9 (1990) 209.
[2] J.P. Parant, R. Olazcuaga, M. Devallete, C. Fouassier, P. Hagenmuller, J. Solid State Chem. 3 (1971) 1.
[3] F. Capitaine, P. Graveau, C. Delmas, Solid State Ionics 89 (1996) 197.
[4] R. Armstrong, P.G. Bruce, Nature 381 (1996) 499.
[5] G. Vitins, K. West, J. Electrochem. Soc. 144 (1997) 3560.
[6] J.M. Paulsen, C.L. Thomas, J.R. Dahn, J. Electrochem. Soc. 146 (1999) 3560.
[7] A. Mendiboure, C. Delmas, P. Hagenmuller, J. Solid State Chem. 57 (1985) 323.
[8] J.M. Paulsen, J.R. Dahn, Solid State Ionics 3 (1999) 126.
[9] Y.U. Jeong, A. Manthiram, J. Solid State Chem. 156 (2001) 331.
[10] A. Caballero, L. Hernán, J. Morales, L. Sánchez, J. Santos Peña, M.A.G. Aranda, J. Mater. Chem. 12 (2002) 1142.
[11] L. Hernán, J. Morales, L. Sánchez, J. Santos, Solid State Ionics 104 (1997) 205.
[12] D.C. Golden, C.C. Chen, J.B. Dixon, Clays Clay Miner. 35 (1987) 271.
[13] S. Bach, J.P. Pereira-Ramos, N. Baffier, J. Electrochem. Soc. 143 (1996) 3429.
[14] S.K. Mishra, G. Ceder, Phys. Rev. B59 (1999) 6120.
[15] S.H. Kim, S.J. Kim, S.M. Oh, Chem. Mater. 11 (1999) 557.
[16] S.H. Kim, W.M. Im, J.K. Hong, S.M. Oh, J. Electrochem. Soc 147 (2000) 413.
[17] K.A. Striebel, C.Z. Deng, S.J. Wen, E.J. Cairns, J. Electrochem. Soc. 143 (1996) 1821.